Journal of Plant Growth Regulation
https://doi.org/10.1007/s00344-024-11301-2

Inactivation Pathway of Diterpenoid Regulator in the Moss *Physcomitrium patens*

Sho Miyazaki[1] · Hiroshi Kawaide[2] · Masatoshi Nakajima[3]

Received: 22 January 2024 / Accepted: 8 March 2024

Abstract

The endogenous levels of plant hormones, including gibberellins (GAs), are strictly regulated and maintained during growth and development in seed plants. The regulation of endogenous levels of bioactive GAs is mediated by the mechanisms of their biosynthesis and inactivation. The moss *Physcomitrium patens* harbors a partial GA biosynthetic pathway from geranylgeranyl diphosphate to *ent*-kaurenoic acid (KA). Recently, we have identified *ent*-3β-hydroxy kaurenoic acid (3OH-KA) as a biologically active metabolite of KA to control the protonemal cell differentiation. In addition, *ent*-2α-hydroxy kaurenoic acid catalyzed by KA 2-oxidase (KA2ox) was also identified as inactive product. Although the activation and inactivation pathways from KA have been identified, the inactivation pathway of 3OH-KA remains to be elucidated. Considering the GA inactivation mechanism of flowering plants, in which GA2ox hydroxylates the C-2 position of GAs as part of the biosynthetic pathway, it was presumed that 3OH-KA was converted to 2,3-dihydroxy KA by PpKA2ox; however, this work shows that PpKA2ox undergoes hydroxylation at the C-16 position to synthesize a new compound *ent*-3β,16β-dihydroxy kaurenoic acid (3,16diOH-KA) from 3OH-KA. The protonemal cell differentiation activity of 3,16diOH-KA was low, and 3,16diOH-KA was detected in wild-type strains. These results indicate that 3,16diOH-KA was the major inactivating metabolite of 3OH-KA.

Keywords Gibberellins · *Physcomitrium patens* · *Ent*-kaurenoic acid · Biosynthesis · 2-Oxoglutarate–dependent dioxygenase

Introduction

Gibberellins (GAs) are involved in various aspects of plant growth and development, including seed germination, stem elongation, and the transition from the vegetative growth phase to flowering (Hedden 2020). The regulation of endogenous levels of bioactive GAs is mediated by the mechanisms of their biosynthesis and inactivation. The most common mechanism for GA inactivation is via 2-oxidation, in which the diterpene GA-backbone is hydroxylated at the C-2β position (MacMillan 2001). The biochemical characterization of the enzymes responsible for 2β-hydroxylation revealed that these enzymes (GA2oxs) belong to the soluble 2-oxoglutarate dependent dioxygenase (2ODD) class (Griggs et al. 1991). GA2oxs can be divided into two groups: C19-GA2ox and C20-GA2ox (Hedden 2020). Bioactive GA, including GA_4 and GA_1, are converted to GA_{34} and GA_8, respectively, by C19-GA2oxs (Fig. 1A). C19-GA2ox hydroxylates the active GA, as well as its precursor, e.g., GA_9, to the inactivated form, GA_{51}. In addition to C19-GA2ox, C20-GA2ox hydroxylates the C-2 position of GAs with 20 carbons, including GA_{12} and GA_{53}, to produce inactive forms GA_{110} and GA_{97}, respectively (Fig. 1A). Thus, C19-GA2ox and C20-GA2ox hydroxylate the C-2 position, regardless of the hydroxy groups at the C-3 or C-13 positions of GA. Plants have acquired a mechanism to precisely fine-tune the levels of bioactive GA during growth and development.

The moss *Physcomitrium patens* harbors a partial GA biosynthetic pathway, from geranylgeranyl diphosphate to *ent*-kaurenoic acid (KA). The KA biosynthesis-deficient

Handling Editor: Theo Lange.

✉ Masatoshi Nakajima
anakajm@g.ecc.u-tokyo.ac.jp

[1] Institute of Global Innovation Research, Tokyo University of Agriculture and Technology, Saiwaicho 3-5-8, Fuchu, Tokyo 183-8509, Japan

[2] Institute of Agriculture, Tokyo University of Agriculture and Technology, Tokyo 183-8509, Japan

[3] Department of Applied Biological Chemistry, The University of Tokyo, Tokyo 113-8657, Japan

Published online: 09 April 2024

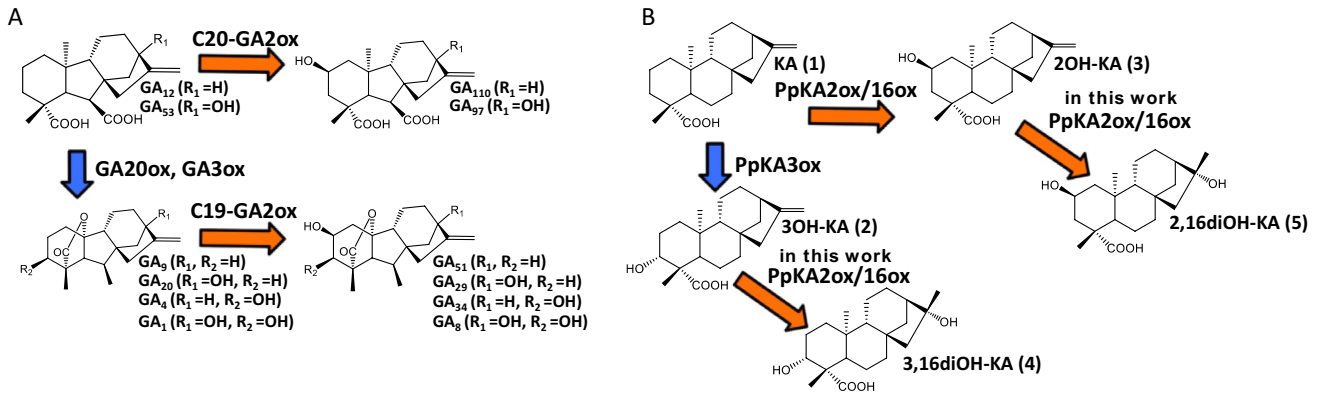

Fig. 1 Major metabolism of GA and 3OH-KA. **A** GA_{12} and GA_{53} are converted to the active form GA_4 and GA_1, respectively, by 2-oxoglutarate-dependent dioxygenases (2ODDs). The activation of GA is mediated by GA 20-oxidase (GA20ox) and GA 3-oxidase (GA3ox), and inactivation is catalyzed by GA 2-oxidase (GA2ox). C19-GA2ox catalyzes the active GA and its precursor (GA_9 and GA_{20}) to form the inactivated form. C20-GA2ox converts GA_{12} and GA_{53} to inactive GA_{110} and GA_{97}, respectively. **B** In *Physcomitrium patens*, KA is activated to form 3OH-KA, which is the final active diterpenoid-type regulator, or inactivated to form 2OH-KA by PpKA2ox. 3OH-KA is inactivated by PpKA2ox (PpKA2ox/16ox) through C-16 oxidation to synthesize a newly identified compound *ent*-3β,16β-dihydroxy kaurenoic acid (3,16diOH-KA). 2OH-KA is also converted to *ent*-2α,16β-dihydroxy kaurenoic acid (2,16diOH-KA) by PpKA2ox (PpKA2ox/16ox)

mutants exhibit defects in protonemal cell differentiation, which are restored by the application of KA but not by GAs. This suggests that KA-derived compounds are potent regulators of protonemal cell differentiation in *P. patens* (Hayashi et al. 2010). Recently, we identified *ent*-3β-hydroxy kaurenoic acid (3OH-KA) as a biologically active metabolite of KA (Fig. 1B, Miyazaki et al. 2018). In addition, *ent*-2α-hydroxy kaurenoic acid (2OH-KA) was identified in *P. patens*; this KA contains a hydroxy group at C-2 and is catalyzed by KA2-oxidase (PpKA2ox) (Fig. 1B). A greater extent of chrolonemata to caulonemata cell differentiation was observed in *P. patens* with 3OH-KA than with KA. Conversely, 2OH-KA possesses no differentiation activity, and no active metabolite has been detected derived from 3OH-KA. This indicates that 3OH-KA is an active regulator, whereas 2OH-KA is the inactive product. Although the KA activation and inactivation pathways have been identified, the metabolic pathways of 3OH-KA remain unclear. Thus, we investigated whether the biologically active compound 3OH-KA was inactivated by PpKA2ox similar to GA inactivation pathway. Our findings revealed that inactivation of C-16 oxidation is facilitated by PpKA2ox, resulting in the synthesis of a new compound, *ent*-3β,16β-dihydroxy kaurenoic acid, from 3OH-KA.

Materials and Methods

Plant Materials and Growth Conditions

Physcomitrium patens Gransden WT strain and *Ppcps/ks* disruption mutant (A74) (Ashton and Cove 1977; Hayashi et al. 2010) were used. *P. patens* was grown on BCDATG medium under standard white light conditions, as described previously (Hayashi et al. 2010). Bioassays of KA and its metabolites were prepared under red light conditions as described previously (Hayashi et al. 2010).

Chemicals

Deuterium-labeled KA (d_2-KA), KA, and GA_4 were purchased from Prof. L. N. Mander (Australian National University, Canberra, Australia). The *ent*-3β-hydroxy-kaurenoic acid (3OH-KA) was purchased from BioBioPha (Kunming, Yunnan, China) via Namiki Shoji Co. Ltd (Tokyo, Japan). The *ent*-2α-hydroxy-kaurenoic acid was enzymatically synthesized as described previously (Miyazaki et al. 2018).

Bioassay

Samples were reconstituted in 10 µL dimethyl sulfoxide (DMSO), and 1 µL of each sample (final concentration 0.1%) was used in the bioassays. *Physcomitrium. patens* was grown on BCDATG medium under red light for 7 days, and the differentiated protonemal cell area was calculated using ImageJ software (National Institutes of Health), as reported previously (Miyazaki et al. 2019).

Liquid Chromatography Tandem Mass Spectrometry Analysis of 3OH-KA Metabolites

Liquid chromatography-MS/MS analysis was conducted according to the procedures in Miyazaki et al. (2015, 2018). Tandem SIMs were applied at the same *m/z* on both Q1

and Q3 to detect KA-metabolites with $[M-H]^-$ from *m/z* 299 > 299 to *m/z* 350 > 350. To quantify KA and its (di) hydroxy-KAs, the extracts were purified using two solid-phase cartridge columns, as described previously by Miyazaki et al. (2015).

Gas Chromatography Mass Spectrometry Analysis

We used a Gas Chromatography Mass Spectrometry (GC-MS) with a GC (Agilent 6890, Agilent Technology, CA, USA) equipped with a DB-1 capillary column (0.25 mm i.d. 15 m, 0.25 mm film thickness; Agilent Technology) and a mass selective detector (Agilent 5975C MSD, ionization energy at 70 eV). The 3OH-KA and 2OH-KA metabolites were subjected to GC-MS after derivatization with a diazomethane and trimethylsilyl ether solutions (MSTFA, Thermo Fisher Science, MA, USA). The samples were injected by split-less injection under the 1.0 ml min^{-1} flow rate of the carrier He gas and the injector temperature of 250 °C. The column temperature was maintained at 80 °C for 1 min, increased at a rate of 33 °C min^{-1} to 245 °C, and then increased at a rate of 2.5 °C min^{-1} to 280 °C. Each metabolite was identified by comparing its MS fragment pattern and Kovats retention index (KRI) with those of the authentic specimens.

High Resolution-Time of Flight Mass Spectrometer Analysis

Mass spectra were acquired using a JMS-T100LC AccuTOF mass spectrometer (JEOL, Tokyo, Japan) coupled to an Agilent 1100 series instrument (Agilent Technologies, Santa Clara, CA, USA). The flow rate was 0.2 mL min^{-1}. For the MS measurements, ESI was applied in the negative ionization mode. The measurement mass range was set to *m/z* 100–1000. The needle voltage of the negative ionization modes was set to − 2000 V. The temperatures of the vaporizer and orifice 1 were maintained at 250 and 80 °C, respectively. A total of 0.1 ppm sample was injected.

Heterologous Expression

PpKA2ox/16ox was cloned into the pGEX 4T3 vector (GE Healthcare, Little Chalfont, UK) and transformed into *Escherichia coli* strain BL21 (DE3) pLysS (Novagen, Madison, WI, USA), along with the empty vector control. The GST-tagged proteins were prepared as described previously (Miyazaki et al. 2018).

Enzyme Reaction

The GST-tagged protein fraction (100 µL) was incubated with 4 mM 2-oxoglutarate, 4 mM ascorbic acid, 0.5 mM $FeSO_4 \cdot 7H_2O$, and 1 µM substrates at 37 °C for 16 h. The product was extracted three times with ethyl acetate. The ethyl acetate phase was then dried in a vacuum evaporator centrifuge (Iwaki Glass, Chiba, Japan). The residual solid was dissolved in methanol and subjected to liquid chromatography-MS/MS analysis.

Synthesis of Dihydroxy Kaurenoic Acids by PpKA2ox/16ox

To synthesize the products from 3OH-KA and 2OH-KA using PpKA2ox/16ox, 1 mg of the substrate, GST-tagged soluble enzyme, and cofactors were prepared. The reaction was stopped by adding acetonitrile. The acetonitrile was evaporated, the sample was loaded onto an Oasis HLB (100 mg) SPE cartridge oasis column (Waters), washed with 1% (v/v) formic acid in water, and then eluted with 1% (v/v) formic acid in acetonitrile. The elute was evaporated to dryness and dissolved in 10% aqueous methanol. The product was purified using reverse-phase high-performance liquid chromatography (HPLC) as described previously (Miyazaki et al. 2018). As a result, 0.9 mg of 3OH-KA + 18 (t_R 35 ~ 37 min) and 0.6 mg of 2OH-KA + 18 (t_R 31 ~ 33 min) were obtained.

Nuclear Magnetic Resonance Analysis

Spectra for PpKA2ox/16ox product were recorded at 25 °C on a JEOL ECA 600 spectrometer (JEOL, Akishima, Japan). The samples were placed in NMR microtubes (CMS-003; Shigemi, Tokyo, Japan), and the chemical shifts were referenced to trimethylsilane (TMS) at 0 ppm. Structural analysis was performed using heteronuclear single-quantum coherence (HSQC), heteronuclear multiple bond correlation (HMBC), and nuclear Overhauser effect spectroscopy (NOE). The spectra were acquired at 600 MHz using standard experiments in Delta ver. 6 software. Correlations from the NOESY dipole–dipole signals were used to assign the stereochemistry. The acquired 1D ^1H and ^{13}C spectra are shown in Supplemental Information. NMR analysis was performed using the JEOL JNM-A600 FT-NMR system.

Results and Discussion

A recent study revealed that PpKA2ox (Pp3c17_7090V3.4), a member of the 2ODD class of enzymes, converts KA to its inactive form 2OH-KA (Miyazaki et al. 2018). Therefore, we investigated whether the reaction proceeds with the bioactive compound 3OH-KA as the substrate, similar to PpKA2ox catalyzing the hydroxylation of C-2 with KA as the substrate. To elucidate the enzymatic reaction, a soluble recombinant protein fused with glutathione S-transferase

was incubated with 3OH-KA and the cofactors required for 2ODD activity in vitro. The negatively charged ions, stemming from both 3OH-KA (molecular weight 318) and its catabolite, were monitored using liquid chromatography tandem mass spectrometry (LC-ESI-MS/MS) analysis, scanning from m/z 299 > 299 to 350 > 350, which revealed that unmetabolized 3OH-KA at t_R 7.6 min had an *m/z* 317 > 317 $[M-H]^-$ ion (Fig. 2A). Conversely, a possible metabolite candidate was identified at t_R 4.3 min an *m/z* 335 > 335 $[M-H]^-$ ion (3OH-KA + 18); however, it was not found with *m/z* 333 > 333 $[M-H]^-$ ion (3OH-KA + 16) (Fig. 2A). The 18 m/z ions larger than those from 3OH-KA were assumed to participate in skeletal transformation or hydroxylation of the exomethylene moiety. Further analysis was performed using gas chromatography-electron ionization-mass spectrometry (GC-MS). Methyl ester-trimethylsilyl ether derivatization of the catabolite was detected at t_R 9.60 min (KRI 2806) (Fig. 2C). The molecular formula of the product, revealed by time-of-flight mass spectrometry (TOF–MS), was $C_{20}H_{32}O_4$ (*m/z* 335.22223 was identified as a negative ion $[M-H]^-$, calculated for *m/z* 335.2228). To elucidate the structure, the product was enzymatically prepared, and its proton-decoupled carbon-13 nuclear magnetic resonance (^{13}C-NMR) spectrum in $CDCl_3$ revealed 20 carbon signals, including a hydroxy group (C-3) and a carboxylate (C-19), similar to the pattern observed for 3OH-KA (Miyazaki et al. 2018, Supplemental Figs. S1–S3 and Supplemental Table S1). Comparison of proton (^{1}H-) and ^{13}C-NMR spectra of 3OH-KA and the product revealed a chemical shift at the C-16 and C-17 positions of the product compared to those of 3OH-KA, indicating loss of the substrate exomethylene and the presence of a hydroxy group at the C-16 or C-17 position. These results indicated that 3OH-KA+18 was synthesized by the mono-hydroxylation of C-16 or C-17. NOE correlations were observed between H-17 and H-11, and the ^{13}C-NMR spectra were compared with published data of *ent*-kauran-16α-ol and *ent*-kauran-16β-ol, permitting the identification of 3OH-KA+18 (Pyrek 1984; Morris et al. 2005). Notably, a signal at 24.46 ppm for 3OH-KA+18 was similar to that reported in the literature, at 24.52 ppm for C-17 of *ent*-kauran-16β-ol, but differed from C-17 for *ent*-kauran-16α-ol (32.52 ppm) (Pyrek 1984; Morris et al. 2005, Supplemental Table S2). The signal for H-17 of the product 3OH-KA+18 (1.36 ppm) matched that reported for *ent*-kauran-16β-ol (1.36 ppm) and not for *ent*-kauran-16α-ol (1.31 ppm) (Pyrek 1984). Based on NMR spectra data, and compared with previously reported data, 3OH-KA+18 was identified as the new compound *ent*-3β,16β-dihydroxy kaurenoic acid (3,16diOH-KA, Fig. 1B).

Considering the GA inactivation mechanism of flowering plants, in which GA2ox hydroxylates the C-2 position of GAs as part of the biosynthetic pathway, it was hypothesized

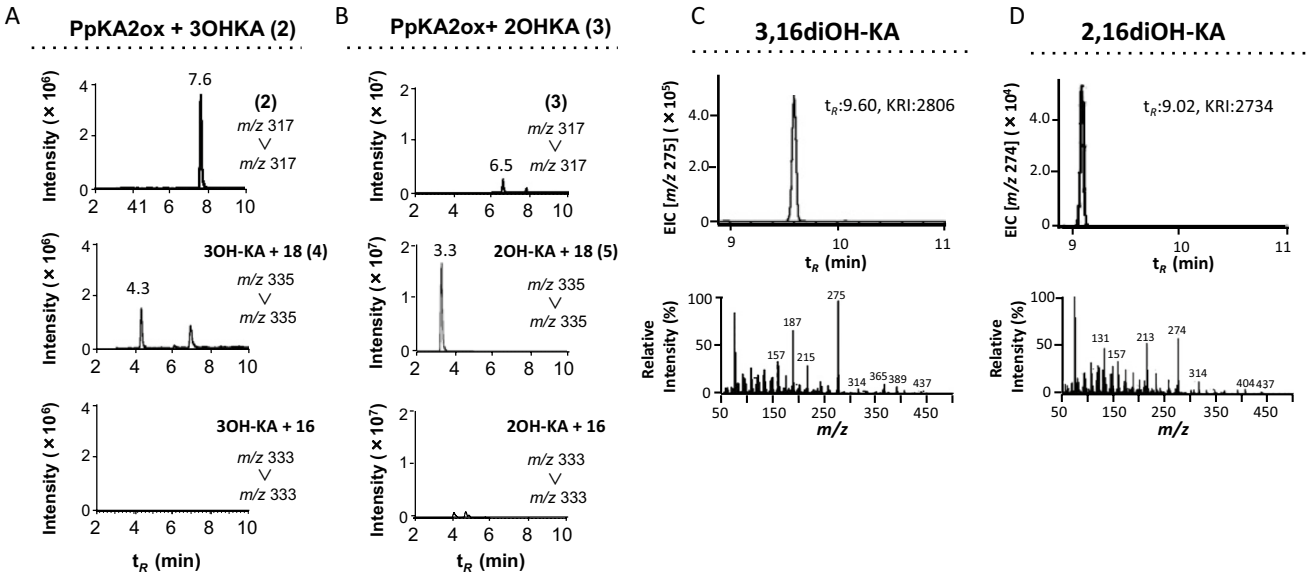

Fig. 2 Identification of metabolites from 3OH-KA and 2OH-KA. **A** Recombinant PpKA2ox/16ox was incubated with 3OH-KA and **B** 2OH-KA, and extracts were analyzed by LC-ESI-MS/MS. LC-ESI-MS/MS analysis detected a metabolite product peak at 4.3 min with an *m/z* 335 > 335 $[M-H]^-$ ion (3OH-KA+18) and at 3.3 min with an *m/z* 335 > 335 $[M-H]^-$ ion (2OH-KA+18), but not with an *m/z* 333 > 333 $[M-H]^-$ ion (3OH-KA+16 and 2OH-KA+16). **C** Gas chromatography-electron ionization-mass spectrometry analysis of 3OH-KA+18 and **D** 2OH-KA+18. The methyl ester-trimethylsilyl ether (Me-TMS) derivatization of 3OH-KA+18 detected at t_R 9.60 min (KRI 2806), and a mass fragment pattern of *m/z* (relative intensity) 275 (100%), 215 (28%), 187 (65%) and 157 (33%). Me-TMS derivatization of 2OH-KA+18 detected at t_R 9.02 min (KRI 2734), with a mass fragment pattern of *m/z* (relative intensity) 274 (63%), 213 (53%), 157 (34%) and 131 (45%)

that 3OH-KA would be converted to 2,3-diOHKA by PpKA2ox; however, PpKA2ox catalyzed hydroxylation at the C-16 position. Therefore, PpKA2ox was confirmed to function as a PpKA2ox/16ox. Previously, we showed that 3OH-KA is the only KA metabolite with physiological activity during protonemal cellular differentiation (Miyazaki et al. 2018). To clarify whether C-16 oxidation of 3OH-KA represents an inactivation step in the metabolism, the biological activities of KA and OH-KAs in the *ent*-kaurene-deficient *P. patens* mutant (*Ppcps/ks*) were compared. As shown in Fig. 3A, The differentiation activity of 3OH-KA at 1 µM was higher than that of KA; however, 2OH-KA and 3,16diOH-KA exerted no biological activity. Next, we measured endogenous 3,16diOH-KA levels via LC–MS/MS analysis in *P. patens*. Subsequently, 3,16diOH-KA as well as 3OH-KA and 2OH-KA were detected in wild-type (WT) stains and in *Ppcps/ks* mutants after addition of KA (Fig. 3B). These results indicated that 3,16diOH-KA was the major inactivating metabolite of 3OH-KA.

C-16-hydroxylated GAs and their synthetic enzymes, which belong to the 2ODD family, have been identified in flowering plants (Xiong et al. 2018; Liu et al. 2019). A GA16 oxidase (GIM2/GAS2, At2g36690) was found to be distantly related to GA-related 2ODD, including PpKA2ox/16ox, via phylogenetic tree analysis (GIM2/GAS2 presented 41.3% sequence identity to PpKA2ox/16ox). Recently, Lange et al. (Lange et al. 2023) concluded that GAS2 is involved in abscisic acid metabolism, which is also consistent with the results of the phylogenetic tree analysis (Kawai et al. 2019). Ishida et al. (Ishida et al. 2022) showed that organically synthesized 16,17-epoxidized GA and 16-hydroxylated GA possess no biological activity in bioassays using rice. The 16,17-epoxidized GA_4 is easily hydrolyzed to 16,17-dihydro-16α,17-dihydroxy GA_4, and its glycoside compound has also been identified in rice (Hasegawa et al. 1994). This suggests that hydroxylation at C-16 controls the activation status of GA, and that the C-16 hydroxide of 3OH-KA may be involved in further metabolic reactions, such as glycosylation, or act as a signaling substance between moss plants.

Since 3OH-KA was oxidized at the C-16 position by PpKA2ox/16ox, we have verified whether a similar reaction proceeded with 2OH-KA as a substrate by PpKA2ox/16ox. As expected, a possible candidate metabolite was detected at t_R 3.3 min and *m/z* 335 > 335 $[M-H]^-$ ion (2OHKA+18), comparable with 3,16diOH-KA, but not at *m/z* 333 > 333 $[M-H]^-$ ion (2OHKA+16) (Fig. 2B). Methyl ester-trimethylsilyl ether derivatization of catabolite 2OH-KA+18 was detected at t_R 9.02 min (KRI 2734) by using GC-MS (Fig. 2D). To determine the structure, the product was enzymatically prepared and analyzed by NMR spectroscopy. The ^{13}C-NMR spectrum revealed 20 carbon signals, including a hydroxy group (C-2) and a carboxylate group (C-19), similar to the pattern observed for 2OH-KA (Miyazaki et al. 2018, Supplemental Figures S4 and S5). Comparing the ^{13}C-NMR spectra of 2OH-KA and 3,16diOH-KA revealed that a signal at 24.49 ppm for C-17 of 2OHKA+18 was analogs to those of 3,16diOH-KA and *ent*-kauran-16β-ol reported previously (Pyrek 1984); however, this differed from C-17 for *ent*-kauran-16α-ol (Morris et al. 2005) (Supplemental Table S3). The 2OHKA+18 was identified as a new compound, termed *ent*-2α,16β-dihydroxy-kaurenoic acid (2,16diOH-KA, Fig. 1B). As shown in Fig. 3A, the protonemal cell differentiation activity of 2,16diOH-KA was

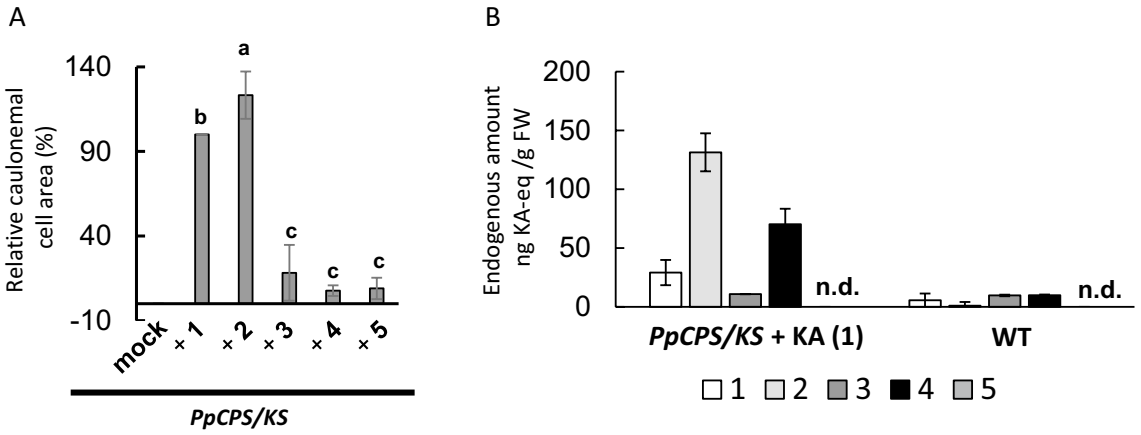

Fig. 3 Bioassay and endogenous amounts of KA metabolites. **A** Bioassay of *Ppcps/ks* protonemal cells on medium containing 1 µM KA (1), 3OH-KA (2), 2OH-KA (3), 3,16diOH-KA (4), and 2,16diOH-KA (5). The relative differentiation ratio was set to 100% when 1 µM KA was added to the medium. Scale bar, 0.1 cm. Bars with different letters indicate significant differences ($p < 0.05$), according to Tukey's HSD test. **B** Endogenous levels of KA (1), 3OH-KA (2), 2OH-KA (3), 3,16diOH-KA (4), and 2,16diOH-KA (5) levels in *Ppcps/ks* and WT plants. After the cultivation of protonemal cells under red light for 7 days, the levels of KA and its metabolites were determined by LC-MS/MS. Error bars indicate ± standard deviation of three biological repeats. *n. d.* not detected

very low and comparable to that of 2OH-KA and 3,16diOH-KA. In contrast to 3,16diOH-KA, 2,16diOH-KA was not detected in *P. patens* (Fig. 3B), suggesting that 2,16diOH-KA was only synthesized in vitro or was metabolized as a glycoside.

The PpKA2ox/16ox was first identified as a C-2 hydroxylase of KA and was shown to oxidize C-16 using 3OH-KA and 2OH-KA as substrates. However, KA+18, in which the C-16 position is hydroxylated when KA is recognized as a substrate, was not detected in vitro (Supplemental Figure S6). Furthermore, PpKA2ox/16ox demonstrated no conversion activity with GA_4 as substrates (Supplemental Figure S6). In flowering plants, GA2ox can hydroxylate the C-2 position of 3OH-GA (e.g., GA_4), and GA3ox can also hydroxylate the C-3 position of 2OH-GA (Watanabe et al. 2021). The PpKA2ox/16ox did not hydroxylate the C-2 position when a hydroxy group was present on the A-ring and targeted the spatially distant D-ring exo-methylene. Since KA+18 was not detected, further studies are needed to determine the physiological significance of KA inactivation by hydroxylation at the C-2 position (+16) and inactivation by hydroxylation of 3OH- or 2OH-KA at C-16 (+18). The PpKA2ox/16ox homologs have been identified in mosses, but not in other bryophytes, ferns, or flowering plants (Nakajima et al. 2020). Phylogenetic analysis has revealed that PpKA2ox/16ox evolved from a common ancestor before diverging from GA2ox and GA3ox (Nakajima et al. 2020). The 2β-hydroxy GAs are not produced in lycophytes or ferns, and GA2ox genes are present in seed plants (Huang et al. 2015), suggesting that functional GA2ox genes evolved later than other GA-related 2ODDs (Hedden 2020). The C-13 hydroxylated GA also functions in the GA biosynthetic pathway; therefore, the substrate recognition pockets of GA-20ox, -2ox, and -3ox should be large. The loose substrate-recognition ability of PpKA2ox/16ox to hydroxylate C-2 and C-16 positions suggests that PpKA2ox/16ox may be a primitive ancestor of GA-inactivating enzymes. The loose substrate-recognition enzyme, which hydroxylates multiple positions on the substrate, may allow the enzyme to adapt to diverse metabolic pathways in the evolutionary process.

Supplementary Information The online version contains supplementary material available at https://doi.org/10.1007/s00344-024-11301-2.

Acknowledgements We thank Dr. Kazuo Furihata and Dr. Kenji Tomita for their helpful discussions on the NMR analysis. This study was supported by the Japan Society for the Promotion of Science (JSPS) KAKENHI Grants 24380060/15H04492 to Masatoshi Nakajima and Hiroshi Kawaide and 16K18693 to Sho Miyazaki, the Moritani scholarship foundation to Sho Miyazaki, and the Wada Kunko-kai research foundation to Masatoshi Nakajima.

Author Contributions Sho Miyazaki designed the study, performed the experiments, collected and analyzed the data, and wrote and revised the manuscript. Masatoshi Nakajima designed the study, analyzed the data, and revised the manuscript. Hiroshi Kawaide revised the manuscript.

Funding Open Access funding provided by The University of Tokyo. This work was funded by the Japan Society for the Promotion of Science (Grant Nos. 24380060, 15H04492), the Moritani Scholarship Foundation, Wada Kunko-kai Research Foundation.

Declarations

Conflict of interest The authors have no competing interests to declare that are relevant to the content of this article.

References

Ashton NW, Cove DJ (1977) The isolation and preliminary characterisation of auxotrophic and analogue resistant mutants of the moss, *Physcomitrella patens*. Molec Gen Genet 154:87–95. https://doi.org/10.1007/BF00265581

Griggs DL, Hedden P, Lazarus CM (1991) Partial purification of two gibberellin 2β-hydroxylases from cotyledons of *Phaseolus vulgaris*. Phytochemistry 30:2507–2512. https://doi.org/10.1016/0031-9422(91)85090-M

Hasegawa M, Nakajima M, Takeda K, Yamaguchi I, Murofushi N (1994) A novel gibberellin glucoside 16α,17-dihydroxy-16,17-dihydrogibberellin A_4-17-O-β-D-glucopyranoside, from rice anthers. Phytochemistry 37:629–634. https://doi.org/10.1016/S0031-9422(00)90329-7

Hayashi K, Horie K, Hiwatashi Y, Kawaide H, Yamaguchi S, Hanada A, Nakashima T, Nakajima M, Mander LN, Yamane H et al (2010) Endogenous diterpenes derived from *ent*-kaurene, a common gibberellin precursor, regulate protonema differentiation of the moss *Physcomitrella patens*. Plant Physiol 153:1085–1097. https://doi.org/10.1104/pp.110.157909

Hedden P (2020) The current status of research on gibberellin biosynthesis. Plant Cell Physiol 61:1832–1849. https://doi.org/10.1093/pcp/pcaa092

Huang Y, Wang X, Ge S, Rao GY (2015) Divergence and adaptive evolution of the gibberellin oxidase genes in plants. BMC Evol Biol 15:207. https://doi.org/10.1186/s12862-015-0490-2

Ishida T, Watanabe B, Mashiguchi K, Yamaguchi S (2022) Synthesis and structure–activity relationship of 16,17-modified gibberellin derivatives. Phytochem Lett 49:162–166. https://doi.org/10.1016/j.phytol.2022.03.022

Kawai Y, Ono E, Mizutani M (2014) Evolution and diversity of the 2–oxoglutarate-dependent dioxygenase superfamily in plants. Plant J 78(2):328–343. https://doi.org/10.1111/tpj.12479

Lange T, Atiq N, Pimenta Lange MJP (2023) *GAS2* encodes a 2-oxoglutarate dependent dioxygenase involved in ABA catabolism. Nat Commun 14:7602. https://doi.org/10.1038/s41467-023-43187-1

Liu H, Guo SY, Lu MH, Zhang Y, Li JH, Wang W, Wang P, Zhang J, Hu Z, Li L et al (2019) Biosynthesis of $DHGA_{12}$ and its roles

in *Arabidopsis* seedling establishment. Nat Commun 10:1768. https://doi.org/10.1038/s41467-019-09467-5

MacMillan J (2001) Occurrence of gibberellins in vascular plants, fungi, and bacteria. J Plant Growth Regul 20:387–442. https://doi.org/10.1007/s003440010038

Miyazaki S, Kimura H, Natsume M, Asami T, Hayashi KI, Kawaide H, Nakajima M (2015) Analysis of *ent*-kaurenoic acid by ultra-performance liquid chromatography-tandem mass spectrometry. Biochem Biophys Rep 2:103–107. https://doi.org/10.1016/j.bbrep.2015.05.010

Miyazaki S, Hara M, Ito S, Tanaka K, Asami T, Hayashi KI, Kawaide H, Nakajima M (2018) An ancestral gibberellin in a moss *Physcomitrella patens*. Mol Plant 11:1097–1100. https://doi.org/10.1016/j.molp.2018.03.010

Miyazaki S, Nakajima M, Kawaide H (2019) Assays of protonemal growth responses in *Physcomitrella patens* under blue- and red-light stimuli. Methods Mol Biol 1924:35–43. https://doi.org/10.1007/978-1-4939-9015-3_4

Morris BD, Foster SP, Grugel S, Grugel S, Charlet LD (2005) Isolation of the diterpenoids, *ent*-kauran-16a-ol and *ent*-atisan-16a-ol, from sunflowers, as oviposition stimulants for the banded sunflower moth, *Cochylis hospes*. J Chem Ecol 31:89–102

Nakajima M, Miyazaki S, Kawaide H (2020) Hormonal diterpenoids distinct to gibberellins regulate protonema differentiation in the moss *Physcomitrium patens*. Plant Cell Physiol 61:1861–1868. https://doi.org/10.1093/pcp/pcaa129

Pyrek JS (1984) Neutral diterpenoids of *Helianthus annuus*. J Nat Prod 47:822–827. https://doi.org/10.1021/np50035a012

Watanabe D, Takahashi I, Jaroensanti-Tanaka N, Miyazaki S, Jiang K, Nakayasu M, Wada M, Asami T, Mizutani M, Okada K, Nakajima M (2021) The apple gene responsible for columnar tree shape reduces the abundance of biologically active gibberellin. Plant J 105:1026–1034. https://doi.org/10.1111/tpj.15084

Xiong W, Ye TT, Yao X, Liu X, Ma S, Chen X, Chen ML, Feng YQ, Wu Y (2018) The dioxygenase GIM2 functions in seed germination by altering gibberellin production in *Arabidopsis*. J Integr Plant Biol 60:276–291. https://doi.org/10.1111/jipb.12619